MAPLE DEPOSITION OF PLGA MICRO- AND NANOPARTICLES EMBEDDED INTO POLYMERIC COATINGS

G. SOCOL[a], N. PREDA[b], M. SOCOL[b], L. SIMA[c], C. R. LUCULESCU[a], F. SIMA[a], M. MIROIU[a], E. AXENTE[a], A. VISAN[a], N. STEFAN[a], R. CRISTESCU[a], G. DORCIOMAN[a], A. STANCULESCU[b], L. RADULESCU[d], I.N. MIHAILESCU[a]

[a]*National Institute for Lasers, Plasma and Radiation Physics, Magurele, Ilfov, Romania*
[b]*National Institute of Materials Physics, Magurele, Ilfov, Romania*
[c]*Institute of Biochemistry, Splaiul Independentei 296, Bucharest, Romania*
[d]*Institute of Cellular Biology and Pathology "N. Simionescu", Bucharest, Romania*

We report the film deposition of Poly(D,L-lactide-co-glycolide) (PLGA) particle systems by matrix assisted pulsed laser evaporation (MAPLE) technique. PLGA+polyvinyl alcohol (PVA), PLGA+PVA+ bovine serum albumin (BSA) and PLGA+PVA+chitosan (CH) nanoparticles were prepared by an oil-in-water emulsion-diffusion-evaporation method. The average diameter of PLGA particles was between 180-250 nm. The coatings were obtained by laser evaporation of frozen targets prepared by mixing appropriate PLGA aqueous suspensions and dimethyl sulfoxide (DMSO) in three ratios. Depending on the DMSO content, we deposited PLGA particles embedded into polymeric layer mainly obtained due to the entirely or partially dissolving of nanoparticles into the initial solution. In vitro results showed that the distribution and morphology of osteoblast-like SaOs-2 cells on some PLGA particle coatings were similar with that of the positive control. The purpose of this study was to develop layers of PLGA particles for local controlled drug delivery.

(Received January 30, 2013; Accepted April 8, 2013)

Keywords: PLGA, chitosan, BSA, nanoparticles, MAPLE

1. Introduction

PLGA is one of the most common biodegradable and biocompatible polymer, approved for human use by U.S. FDA. PLGA nano- or microparticles can serve as delivery systems for various active agents (e.g. anticancer, vitamins, proteins, drugs, growth factors, etc.) [1-7]. PLGA degrades through hydrolysis processes and produces carboxylic acids [8], which further accelerate the degradation of PLGA according to the acid catalyzed hydrolysis mechanism [9]. A high acidic environment can induce the aggregation and denaturation of sensitive compounds like proteins. Therefore, the hydrolysis mechanisms of PLGA particles can be tailored by addition of chitosan in their composition [5].

Chitosan (CH) is a natural linear polysaccharide derived by deacetylation of chitin. Furthermore, it is considered a cationic polymer, biodegradable, biocompatible and nontoxic. Chitosan is a hydrophilic polymer which dissolves in aqueous solution with pH below 5.5. Owing to its amino functional groups, chitosan has been comprehensively investigated in the drug and gene delivery or biomedical applications [2,6, 10]. The most distinctive characteristics of chitosan are its unique biocompatibility and biodegradability, which recommend it for biomedical and pharmaceutical exploitation.

*Corresponding author: gabriel.socol@inflpr.ro

Bovine serum albumin (BSA) is a compound often applied for modeling of highly water soluble protein agents [11, 12]. PLGA–BSA composite nano- and microparticles were efficiently fabricated by the water-in-oil-in-water (w/o/w) double emulsion method [13].

Particle size, encapsulation efficiency and structure were proved to be important formulation properties. Their size and structure influence the release kinetics and interaction with cells or tissues. These properties and the relationships between them were frequently reported for particle systems where the polyvinyl alcohol was used as emulsifier in the external water phase [13]. The degree of toxicity of such polymeric particles is strongly influenced by the biological environment and local conditions, which can alter their degradation rate or release kinetics.

Despite the great progress concerning mainly PLGA microspheres synthesis and properties reported recently in the literature [14, 15] there is a big gap related to their deposition and characterization in form of thin films for biomedical applications. Only few techniques so far, like electrophoretic deposition, layer by layer, etc were employed for deposition of PLGA particle coatings the main limitation being related to poor particles-substrate adhesion[16, 17]. Matrix assisted pulsed laser evaporation (MAPLE) has proved to be a powerful technique for deposition of organic compounds [18-21] as well as nanoparticle layers of inorganic compounds [19]. A particular interest for application arises from the development of PLGA coatings for local and targeted delivery. The goal of our study was to exploit the MAPLE technique advantages for deposition of PLGA particles coatings as well as nano- or microparticles embedded in polymeric matrix due to their increase adhesion to the substrate.

2. Materials and methods

2.1 Reagents and chemicals

Poly(lactide-co-glycolide) (PLGA) with a monomer ratio [lactic acid/glycolic acid] of 75/25, molecular weight (MW) of 76-115 kDa, medium molecular weight chitosan, polyvinyl alcohol (PVA) with average MW of 146-186kDa, 99+% hydrolyzed and bovine serum albumin (BSA, fraction V) and chitosan (CH, medium molecular weight) were purchased from Sigma–Aldrich. All other chemicals (ethyl acetate, ethanol, acetone, DMSO) were of analytical grade while the water was always deionized.

The coatings were deposited on soda lime glass and IR transparent (100) double side polished silicon, both with 10×10 mm^2 size.

2.2 Nanoparticles preparation

PLGA, BSA-PLGA and CH-PLGA nanoparticles were prepared by an oil-in-water emulsion-diffusion-evaporation technique as described before [13]. Briefly, initial solutions of PLGA in ethyl acetate (20 mg/ml) and PVA in deionized water (10 mg/ml) were prepared. 5 ml of PVA aqueous solution were used in order to dissolve 100 mg BSA or 30 mg chitosan. Three emulsions were obtained by mixing the following volumes: a) 5 ml PLGA and 5 ml PVA in 90 ml water; b) 5 ml PLGA and 5 ml PVA containing BSA in 90 ml water; c) 5 ml PLGA and 5 ml PVA containing chitosan in 90 ml water. All the systems were successively ultrasonicated for 3 minutes at 130 W for 50 % amplitude using a Sonics Ultracell, stirred at room temperature for 3 hours, centrifuged at 4500 rpm for 15 minutes and then washed three times with deionized water. Next abbreviations will be used throughout the text as reference for the different particle systems, *PP* for PLGA+PVA, *PPB* for PLGA +PVA+ BSA and *PPC* for PLGA+PVA+CH.

2.3 MAPLE deposition of PLGA particle coatings

The focused radiation of a KrF* (λ = 248 nm, τ_{FWHM} = 25 ns) laser source (model COMPexPro 205, Lambda Physics-Coherent) impinged the frozen targets at an angle of 45°. The layers were grown by applying 30,000 subsequent laser pulses at a laser fluence of 650 mJ/cm^2 and a repetition rate of 20 Hz. For each PLGA particle system (PP, PPB and PPC), three solutions were prepared by mixing appropriate PLGA aqueous suspensions with different amounts of

DMSO (Table I). Then, solid targets were obtained by freezing the PLGA mixtures at liquid nitrogen temperature. During the laser irradiation, the targets were maintained at low temperature by liquid nitrogen cooling. Thus, three batches of samples were deposited using PP, PPB and PPC micro- and nanoparticles (Table I). Prior to introduction inside the deposition chamber, the substrates were ultrasonically cleaned with acetone, ethanol and deionized water for 15 mins and then dried in a jet of high purity nitrogen. All the depositions were conducted at a background pressure of 2 Pa while the glass and silicon substrates were rotated to improve the uniformity of PLGA coatings. MAPLE depositions were carried out at room temperature and at a target-substrate separation distance of 4 cm.

Table I. Ratios of DMSO and PLGA aqueous suspensions used for target preparation

Sample	Particle system	Ratio of particle aqueous suspension	DMSO Ratio/concentration
PP1	PLGA/PVA	5/6	1/6
PPB1	PLGA/PVA/BSA	5/6	1/6
PPC1	PLGA/PVA /CH	5/6	1/6
PP2	PLGA/PVA	19/20	1/20
PPB2	PLGA/PVA/BSA	19/20	1/20
PPC2	PLGA/PVA /CH	19/20	1/20
PP3	PLGA/PVA	29/30	1/30
PPB3	PLGA/PVA/BSA	29/30	1/30
PPC3	PLGA/PVA /CH	29/30	1/30

2.4 Fourier transform infrared (FTIR) spectroscopy

Transmission FTIR spectra of PLGA particle dropcasts and films were measured using a FTIR spectrophotometer (Shimadzu 8400S, Japan) while the PLGA, PVA, BSA and PVA powder spectras were collected by a diffuse reflectance accessory. For each type of powder an amount of 2% (w/w) in respect to potassium bromide (KBr), was mixed with dry KBr into fine powder by means of an agate mortar. The dropcasts were prepared by pouring of few droplets from the initial aqueous particle suspension on IR transparent double side polished silicon wafers. In the case of particle coatings and dropcasts spectra, the contribution of Si substrate was subtracted when the background was collected. The spectra were obtained by accumulating 40 scans in the range 4000–400 cm^{-1} with a resolution of 4 cm^{-1}.

2.5 Morphological studies

The morphological features of PLGA particle dropcasts and MAPLE films were examined by Atomic Force Microscopy (AFM) in tapping mode with a Nanonics MV 4000 Microscope. Scanning Electron Microscopy (SEM) investigations were performed with a FEI Co., model Inspect S microscope, working distance 0-30 mm and a maximum accelerating voltage of 30 kV. Particles size and their distribution was determined by processing the SEM micrographs with ImageJ software.

2.6 Microscopic assessment of bone cells and PLGA coatings

Osteosarcoma (SaOs-2) cells were cultured in DMEM supplemented with 10% FCS (Biochrom AG), 1% Glutamax, 50 U mL-1 penicillin, and 50 mg mL-1 streptomycin (Gibco), in a 5% CO2 humid atmosphere at 37°C. Each sample was seeded with 50 000 cells grown for 72 h in complete media. The viability and the morphology of SaOs-2 cells on the PLGA coatings were assesed by a Nikon Eclipse E600W epifluorescence microscope equipped with a differential interference contrast (DIC) module for Nomarski illumination, used to enhance the contrast in

unstained, transparent samples at a magnitude of 100x. Fluorescence microscopy (530nm filter) was used to evaluate the distribution of polymeric aggregates and microparticles on the surface of investigated coatings. Pictures were taken using a Nikon Digital Light DS-SM camera and NIS-Elements BR Software. DIC and green fluorescence merged images were processed using Adobe Photoshop.

3. Results and discussion

3.1 FTIR composition of PLGA coatings

In the Fig. 1 are given the FTIR spectra of PVA, PLGA, BSA and CH powders whereas in the figure 2 are presented the FTIR spectras of the MAPLE films and dropcasts, respectively. In the figure 2 right, we showed only the FTIR spectra of PLGA coatings deposited from the targets with the highest DMSO content. The thickness of the films strongly decreases with the decrease of DMSO concentration (data not shown). Unlike DMSO, water is characterized by a low optical absorption at the employed laser wavelength (248 nm). Thus, the laser evaporation efficiency of the frozen matrix solution (DMSO+ water) increases with the DMSO content. Therefore, we presented the FTIR spectra of thicker samples because a better IR signal was collected.

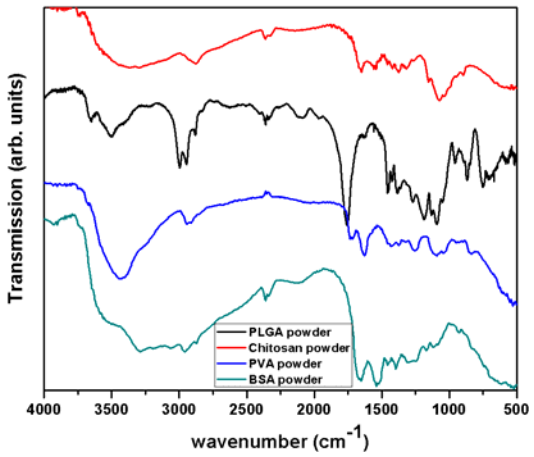

Fig. 1 FTIR spectra of PLGA, CH, PVA and BSA powders

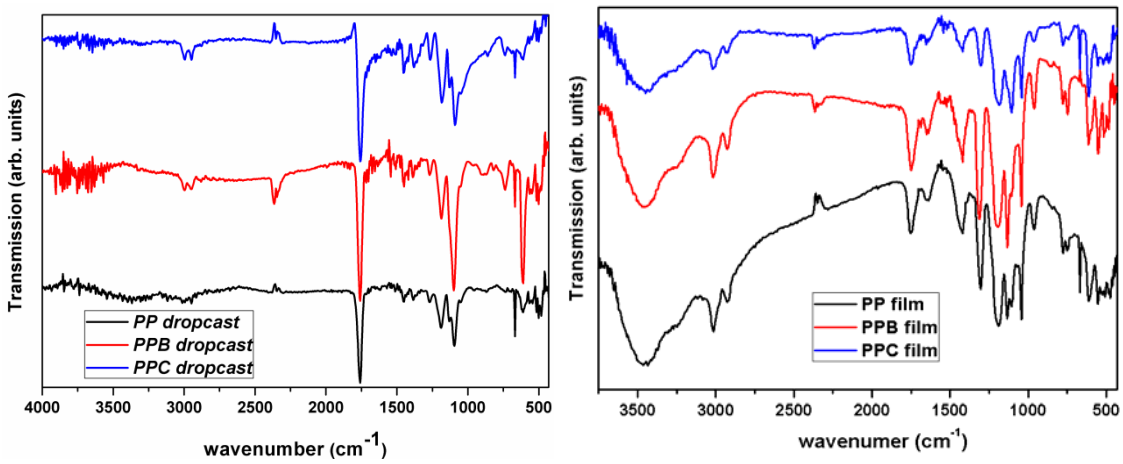

Fig. 2 FTIR spectra of PP, PPB and PPB dropcasts (left) and coatings (right)

The FTIR spectra of PLGA and PVA, CH samples have similar characteristic peaks, since they basically have the same functional groups. Therefore, all the films present similar peaks. A broad band at 3100-3600 cm^{-1} appears due to the overlapping bands of O-H stretching of PVA and the vibration of OH terminal groups in PLGA. The bands at 3014 and 2922 cm^{-1} were assigned to C-H stretch of -CH_2 bond. The strong band at 1754 cm-1 was attributed to C=O bond of the ester group. The peaks at 1419 and 1654 cm^{-1} could be assigned to the carbon–carbon (C=C) double bonds while the peaks between 1194-1131 cm^{-1} were assigned to C-O stretch. The perpendicular band at 1340 cm^{-1} could also be related to the hydroxyl group, which shifts to 1311cm^{-1} due to the hydrogen bonding between PVA and PLGA chains. The peaks between 775 and 611 cm^{-1} is assigned to CH-bend.

The bands at 1040 and 960 cm^{-1} are given by Si-O-Si vibration and Si-O stretch due to native oxide on the surface of Si substrate.

Typical peaks around 1650 cm^{-1} and 1540 cm^{-1} characteristic to amine I and amine II bands of BSA are not clearly seen in case of PPB films or dropcasts because they were submerged in the strong peaks of the polymeric matrix.

These results proved us that the PLGA systems were transferred by MAPLE technique without altering the initial composition.

3.2 Size and morphology

Fig. 3 depicts typical SEM micrographs for PP, PPB and PPC micro- and nanoparticle dropcasts. SEM images of PLGA particles systems show homogeneous and spherical-shaped particles in nano- and micrometric range. All the particles present smooth surface and regulated shape. More than 90% PP nanoparticles were measured with diameter below 200 nm while the average nanoparticle size was about 180±10 nm. An increase of nanoparticle's diameter was observed when the BSA and CH were incorporated through the nanoparticle synthesis pathway. Thus, the average diameter of PPB and PPC nanoparticles was 230±10 nm and 250±10 nm whereas 90% of the PPB and PPC nanoparticles were with a diameter below 300 nm. In the case of PPC particles, a slight increase of the number and microparticle's diameter was found.

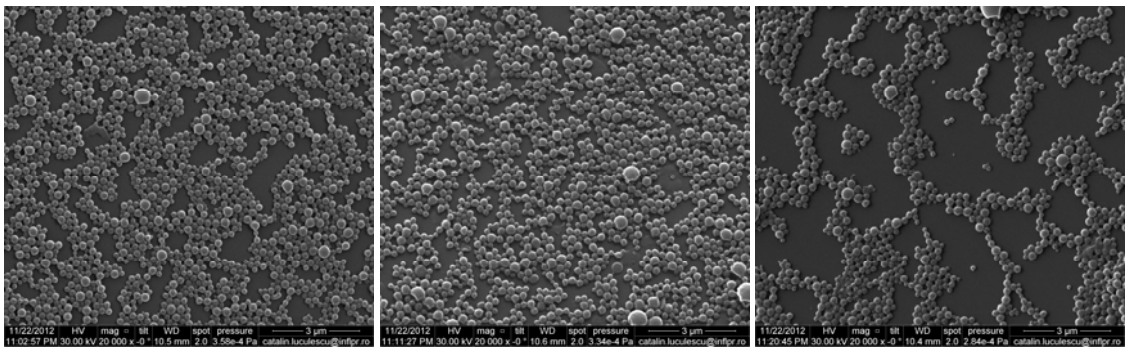

Fig. 3 Typical SEM micrographs of PP (left), PPB (center) and PPC (rigth) dropcasts

AFM images of PLGA dropcasts (fig. 4) confirm the same regulated aggregates with round shape and size distribution observed in SEM micrographs (fig. 3).

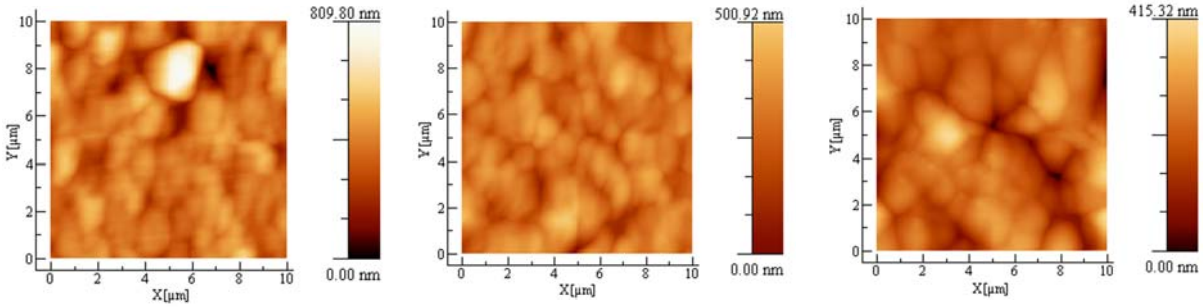

Fig. 4 Typical AFM images of PP (left), PPB (center) and PPC (rigth) dropcasts

Figs. 5 and 6 present selected SEM and AFM images of representative PLGA coatings obtained after MAPLE transfer. Depending of DMSO fractions added to PLGA aqueous suspensions, the structure and integrity of the transferred particles were altered in the same manner. Therefore, independently of the composition of particles, SEM and AFM results evidenced similar morphologies of coatings deposited at the same MAPLE conditions and DMSO concentrations.

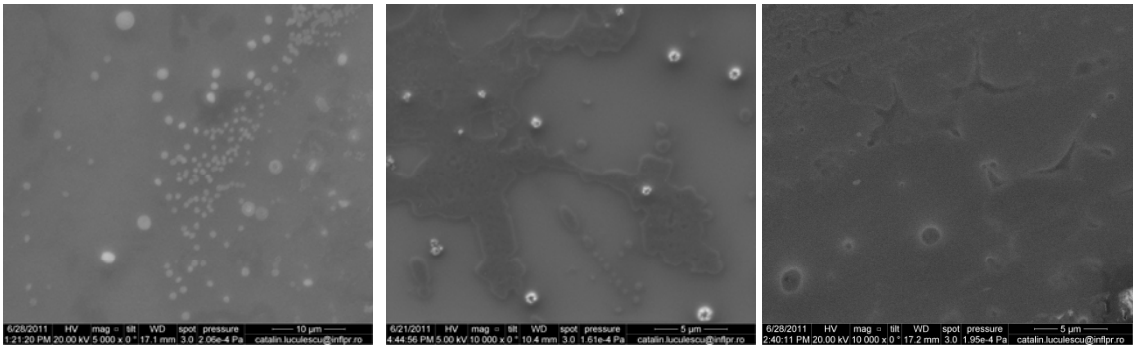

Fig. 5 Selected SEM micrographs of PP3 (left), PPC2 (center) and PPB1 (rigth) coatings

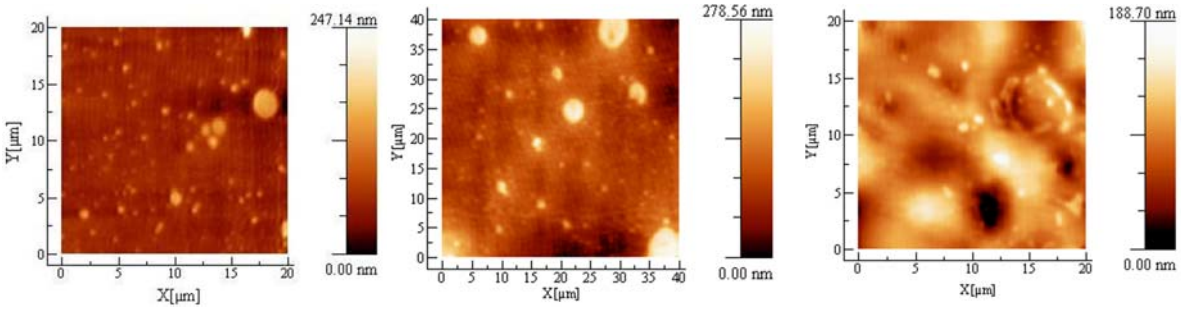

Fig. 6 Selected AFM images of PP3 (left), PPC2 (center) and PPB1 (rigth) coatings

At high DMSO concentration (1/6 ratio), the most of PLGA particles were dissolved and a film with a low number of embedded particles was obtained (fig. 5 and 6 right). For these coatings labeled with 1, only the large particles, most of them with micrometric size were visible. However, these PLGA aggregates reveal irregularities in their shape which demonstrates that the structure of particles was strongly altered. We assumed that PLGA nanoparticles were entirely dissolved and contributed to the formation of PLGA coatings.

At lower concentrations of DMSO (1/20 ratio), a resembling morphology of the coatings was obtained. Nevertheless, the shape of large PLGA particles was less affected while their number increased (figs. 5 and 6 center).

At the lowest DMSO concentration (1/30 ratio), sub-micrometric PLGA particles were visible in AFM and SEM images and only very small nanoparticles were dissolved, (figs. 5 and 6 left). Moreover, the number of particles embedded in the PLGA films was the highest for this particular DMSO concentration (1/30 ratio).

Accordingly, our results have proven that using MAPLE technique, one can tailor the physico-chemical properties of the coatings by simply playing the experimental conditions. Several parameters are involved, as clearly evidenced in our experiments: the nature and the concentration of the solvent in close relationship with absorption at the laser wavelength used in the deposition, as well as the properties of the material to be transferred. Recent simulations of MAPLE process by coarse-grained molecular dynamic evidenced a broad size distribution of the ejected clusters during the complex dynamics of the ejection, transport, and deposition of the polymer molecules to the substrate [22].

3.3 In vitro results

In order to determine the distribution, colonization and morphology of the SaOs-2 cells on PLGA coatings, a parallel observation in both DIC and fluorescence microscopy modes was carried out at 72 hours after starting the culture.

In the figures 7-9 left column the DIC images of SaOs-2 cells grown on PP (fig. 7), PPB (fig. 8) and PPC (fig. 9) coatings are given, while on the second column (center) the fluorescence images for the same PLGA sample fields are presented. Superimposed images obtained through DIC and green fluorescence (530 nm) filter are represented to the right column.

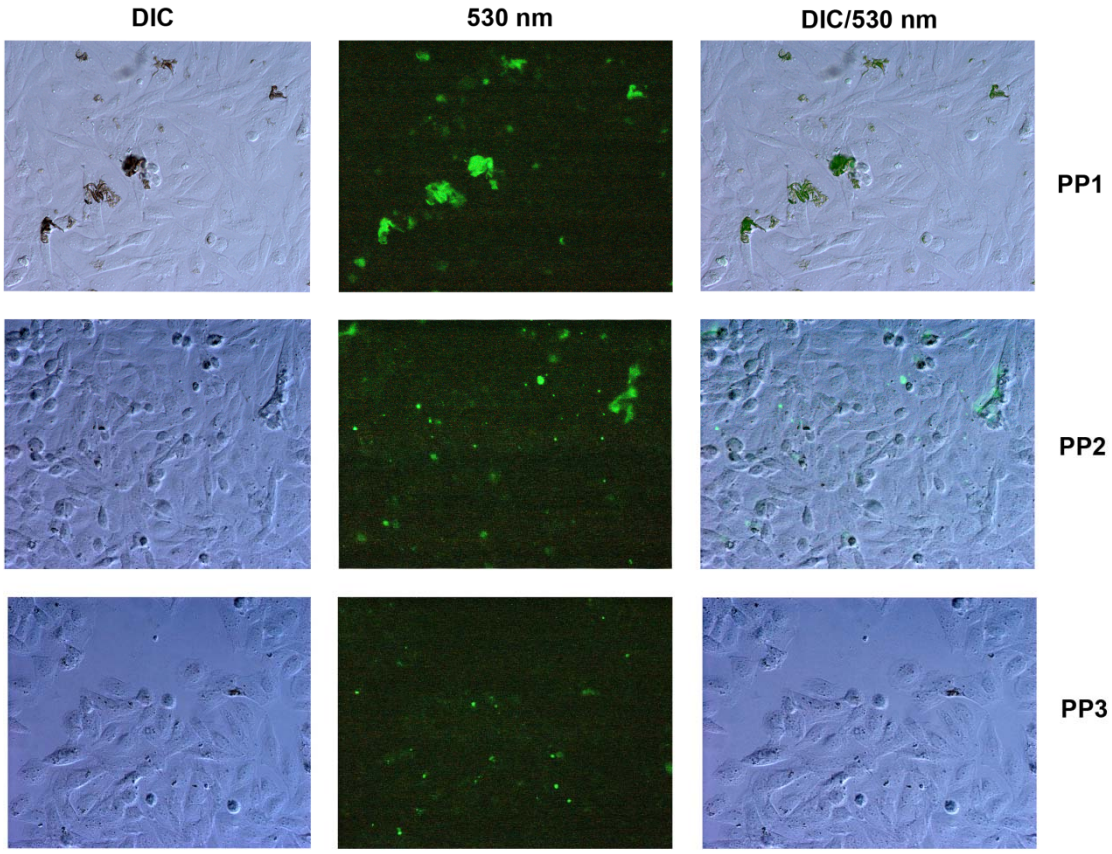

Fig. 7 Left column shows DIC microscope images of SaOs-2 cells morphology while center column presents fluorescence microscope images of large polymeric aggregates on PP coatings. In the right colum are given the superimposed images of DIC and green fluorescence at (530 nm) filter.

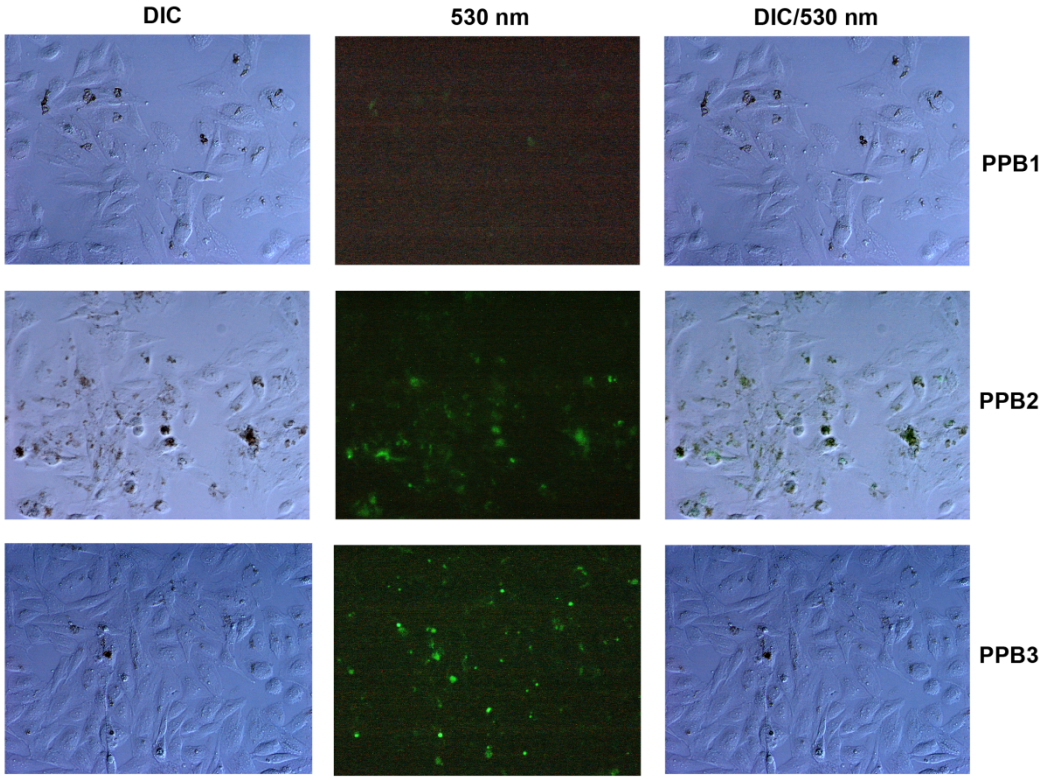

Fig. 8 Left column shows DIC microscope images of SaOs-2 cells morphology while right column presents fluorescence microscope images of large polymeric aggregates on PPB coatings. In the right column are given the superimposed images of DIC and green fluorescence at (530 nm) filter.

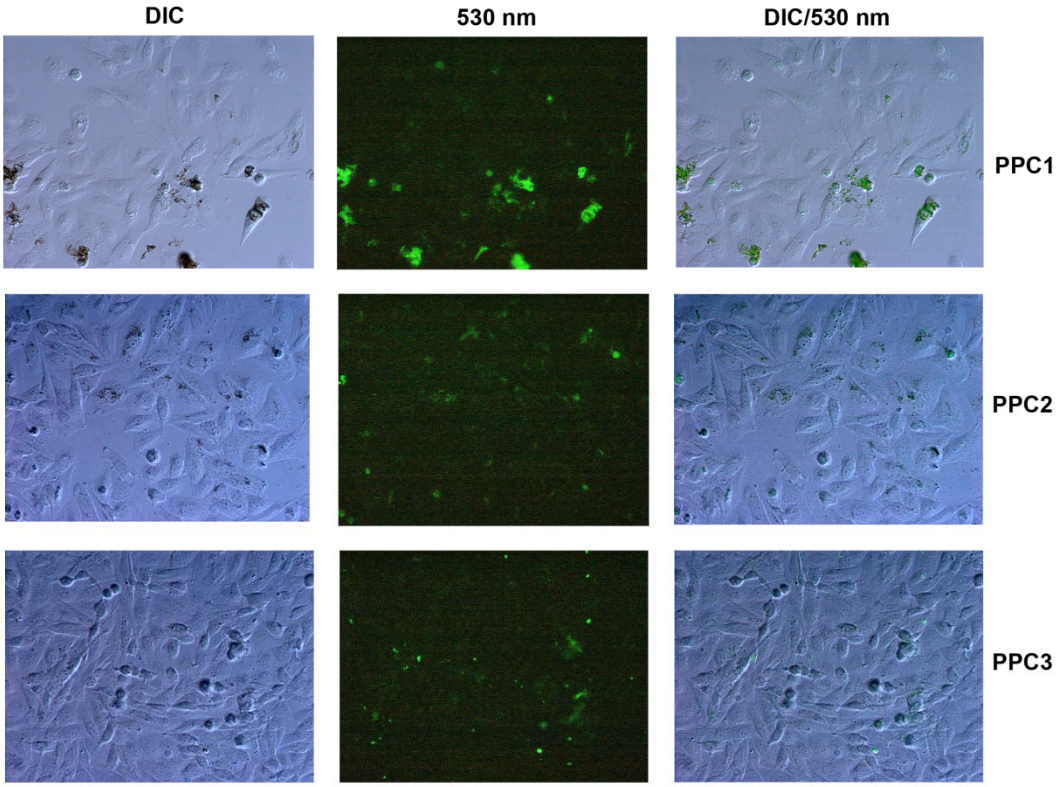

Fig. 9 Left column shows DIC microscope images of SaOs-2 cells morphology while right column presents fluorescence microscope images of large polymeric aggregates on PPC coatings. In the right column are given the superimposed images of DIC and green fluorescence at (530 nm) filter.

Analysis of cells cultured on each PLGA coating showed a different density reached after interaction with nanoparticles, depending on the initial DMSO concentration from the targets and PLGA system (PP, PPB or PPC).

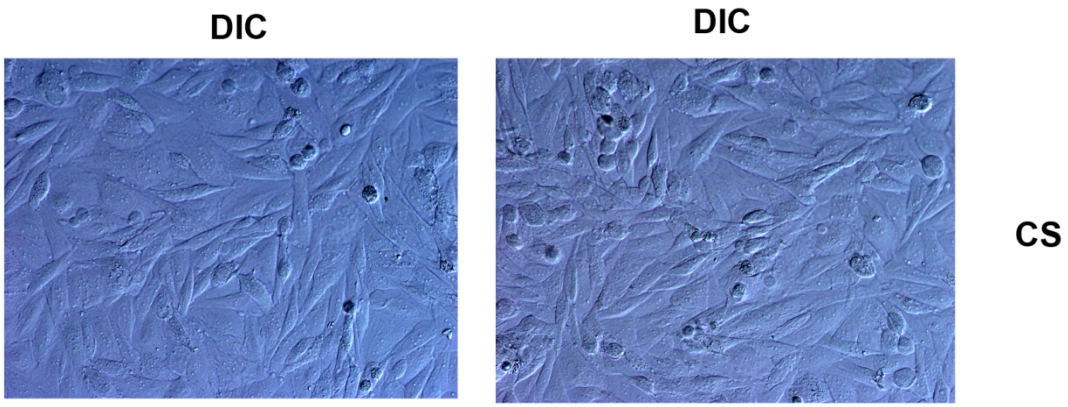

Fig. 10 DIC microscope images show SaOs-2 cells distribution on positive control – microscopy cover slips.

It was observed that the cell spreading and cell morphology on the PP1, PP2, PPC2, PPB3 and PPC3 coatings were comparable to the control (fig. 10). This can indicate that the cell viability remained high after being in contact with the particular surface topology and composition of these polymeric coatings. On the same samples, the cells were elongated as well as very well attached and spread over the whole surface, while on other films (PP3, PPB1, PPB2, PPC1) the SaOs-2 cells were arranged in an irregular non-homogeneous distribution, and associated in clusters mainly where the larger PLGA aggregates were found on the films. However, the difference in morphology observed for the cells grown on these three types of polymeric systems was not dramatic and further more in-depth studies are required to confirm and complete the results.

4. Conclusions

MAPLE has proved an attractive deposition technique due its versatility in terms of the stoichiometric transfer of a broad range of compounds and the control at the nano- and micrometric scale. We showed that PLGA particles can be transferred in form of particles embedded into a polymeric matrix by MAPLE technique without altering their initial composition. At very low DMSO concentrations (1/30) the PLGA micro- and large nanoparticles were embedded in the polymeric layer whereas at high DMSO concentrations almost all the PLGA nanoparticles were dissolved and further contributed at the formation of polymeric layer. Biocompatibility assay showed that nanoparticles films are not cytotoxic for bone cells, which encourages further assessment of this type of biomaterials for their application in drug release at implantation sites. Minor differences observed between various PLGA-based structures taking as readout cell density are to be studied in future cell adhesion and functionality studies.

Acknowledgments

Human osteosarcoma SaOs2 cells were a kind gift from Dr. Karine Anselme, IS2M, Mulhouse, France. G. Socol, F. Sima, L. E. Sima and L. Radulescu acknowledge the financial support from the European Social Fund POSDRU 2007-2013 through the contract POSDRU/89/1.5/S/60746. This work was supported by the Romanian National Authority for Scientific Research, CNCS-UEFISCDI, project number PCCA 153/02.07.2012.

References

[1] Tae Hyung Kim, Hai Hua Jiang, Chan Woong Park, Yu Seok Youn, Seulki Lee, Xiaoyuan Chen, Kang Choon Lee, Journal of Controlled Release **150**, 63 (2011).

[2] S. Taetz, N. Nafee, J. Beisner, K. Piotrowska, C. Baldes, T.E. Mürdter, H. Huwer, M. Schneider, U.F. Schaefer, U. Klotz, C.-M. Lehr, European Journal of Pharmaceutics and Biopharmaceutics **72**, 358 (2009)

[3] Jong-Ho Kim, Ajay Taluja, Kristine Knutson, You Han Bae, Journal of Controlled Release **109,** 86 (2005).

[4] Alexandra Giteau, Marie-Claire Venier-Julienne, Stephane Marchal, Jean-Luc Courthaudon, Michele Sergent, Claudia Montero-Menei, Jean-Michel Verdier, Jean-Pierre Benoit, European Journal of Pharmaceutics and Biopharmaceutics **70**, 127 (2008).

[5] Mingbo Wang, Qingling Feng, Xiaodong Guo, Zhending She, Rongwei Tan, Mingbo Wang, Qingling Feng, Xiaodong Guo, Zhending She, Rongwei Tan, Polymer Degradation and Stability **96**, 107 (2011).

[6] Marco Zaru, Anna Maria Fadd, Sophia G. Antimisiaris, Colloids and Surfaces B: Biointerfaces **67**, 166 (2008).

[7] Sejin Son, Woo Ram Lee, Yoon Ki Joung, Myung Hee Kwon, Yong Sung Kim, Ki Dong Park, International Journal of Pharmaceutics **368**, 178 (2009).

[8] J.H. Kim, A. Taluja, K. Knutson, Y.H. Bae, J Controlled Release;**109,** 86 (2005).

[9] J.M. Bezemer, R. Radersma, D.W. Grijpma, P.J. Dijkstra, CA van Blitterswijk, J. Feijen, J Controlled Release; **67**, 249 (2000).

[10] Noha Nafee, Marc Schneider, Ulrich F. Schaefer, Claus-Michael Lehr, International Journal of Pharmaceutics **381**, 130 (2009).

[11] Kuen Yong Lee, Soon Hong Yuk, Prog. Polym. Sci. **32**, 669 (2007).

[12] Tivadar Feczk, Judit Toth, Janos Gyenis, Colloids and Surfaces A: Physicochem. Eng. Aspects **319,** 188 (2008).

[13] Mei Ling Ho, Yin Chih Fu, Gwo Jaw Wang, Hui Ting Chen, Je Ken Chang, Tsung Hsien Tsai, Chih Kuang Wang, Journal of Controlled Release **128**, 142 (2008).

[14] Oksan Karal-Yilmaz, Abdulkadir Ozkan, Emel Akgun, Manolya Kukut, Kemal Baysal, Timucin Avsar, Turker Kilic, J Mater Sci: Mater Med (2012) DOI 10.1007/s10856-012-4784-2

[15] Yuting Lin, Yan Li, Chui Ping Ooi, J Mater Sci: Mater Med **23,** 2453 (2012). DOI 10.1007/s10856-012-4723-2.

[16] H. N. So, Y. N. Hye, R. J. Jae, S. B. In, & Park, J.-S.. Bull. Korean Chem. Soc. **28**, 397 (2007).

[17] J.M. Barichello, M. Morishita, K. Takayama, T. Nagai. Drug Dev Ind Pharm **25,** 471 (1999).

[18] R. Cristescu, A. Doraiswamy, G. Socol, S. Grigorescu, E. Axente, D. Mihaiescu, A. Moldovan, R. J. Narayan, I. Stamatin, I. N. Mihailescu, B. J. Chisholm, D. B. Chrisey, APPLIED SURFACE SCIENCE, **253(**15), SI, 6476 (2007).

[19] R. Cristescu, A. Doraiswamy, T. Patz, G. Socol, S. Grigorescu, E. Axente, F. Sima, R. J. Narayan, D. Mihaiescu, A. Moldovan, I. Stamatin, I. N. Mihailescu, B. Chisholm, D. B. Chrisey, APPLIED SURFACE SCIENCE, **253**(19), 7702 (2007).

[20] G. Socol, I. N. Mihailescu, A.M. Albu, St. Antohe, F. Stanculescu, A. Stanculescu, L. Mihut, N. Preda, M. Socol and O. Rasoga, Applied Surface Science **255**(10), 5611 (2009)

[21] Anna Paola Caricato, Armando Luches and Roberto Rella, Sensors, **9**(4), 2682 (2009).

[22] L. V. Zhigilei, A. N. Volkov, E. Leveugle, and M. Tabetah, Appl. Phys. A **105**(3), 529 (2011)